Isotropic energy and luminosity correlations with spectral peak energy for five long Gamma-Ray Bursts

Feraol F. Dirirsa[1,*] and Soebur Razzaque[1] on behalf of the *Fermi*-LAT Collaboration

[1]University of Johannesburg, Kingsway Campus, Auckland Park 2006, Johannesburg

E-mail: *fdirirsa@uj.ac.za

Abstract. We present a time-integrated spectral analysis of five long gamma-ray bursts (GRBs) with identified redshift and triggered by the *Fermi* satellite in 2015. Two bursts (GRB150403A & GRB150314A) are detected both by the *Fermi* Large Area Telescope (LAT) and Gamma-Ray Burst Monitor (GBM) while the other three sources (GRB150727A, GRB151027A & GRB150301B) are detected only by the GBM. We describe the observable correlations of these bursts such as the intrinsic peak energy with the isotropic-radiated energy and luminosity in the source frame, to show their consistency with the global Amati/Yonetoku relation. We investigate the possibility that Band function, Power law (PL), Smoothly broken power law (SBPL) and Comptonized components may be present separately by fitting the prompt emission spectra in the keV-MeV energy range. At last, the intrinsic peak energy which is highly correlated to both the radiated isotropic energy (the Amati relation) and the peak luminosity (the Yonetoku relation) in the source frame is summarized.

1. Introduction

Gamma-ray bursts, mostly emitting radiation in the gamma-ray waveband which lasts for few seconds, and may be tailed by the X-ray, optical or radio emission which last for a few days. Those bursts are the most luminous electromagnetic explosions in the Universe [1], with the highest isotropic equivalent radiated energy E_{iso}, up to 10^{54} erg [2]. For long GRBs (duration > 2 s), observational correlations among the rest frame intrinsic spectral peak energy E^{i}_{peak}, the peak isotropic luminosity L_{iso} and the isotropic radiated energy in the prompt emission phase have been anticipated. E^{i}_{peak} correlates with the isotropic luminosity L_{iso} (so called Yonetoku relation) [3] and with the isotropic radiated energy first stated by Amati et al. [4]. One of the key properties of the prompt emission of GRBs that is still poorly understood concerns the spectral-energy correlations found when considering the time-integrated spectra of bursts of known redshift. After measuring the redshift of GRB, one can correct for cosmological effects and infer its rest frame photon energy E^{i}_{peak}, in a νF_{ν} representation. An open issue is that if these relations have a physical origin or they are due to instrumental selection effects (or biases) which was argued by many authors [5, 6, 7]. The strong motivation to investigate the correlations of GRB phenomenology can be used to make GRBs into standard candles of cosmology, alongside the commonly used standard candle, the supernovae Type Ia for the purpose of constraining the cosmological parameters and to understand the GRB physics of the prompt emission.

In this work, we discussed the E_{iso} and L_{iso} correlations with E^{i}_{peak} for five long GRBs with identified redshift z detected by *Fermi* in 2015 (*Fermi*-2015). Our analysis is based on GRB

time-integrated spectra. Since, the spectra of GRBs are in a wide energy range, it can usually be described by the Band function [8], which is a two smoothly jointed power laws cutting at a breaking energy. Below the breaking energy, the Band function reduces to a cut-off power law, while above the breaking energy [8], it is a simple power law. Further, since the prompt emission spectra of the *Fermi*-GBM GRBs covers large energy range, their spectra can be fitted well even using a power law with exponential high-energy cut-off (Comptonized) and SBPL model. Using the parameters employed in the best-fit spectral model, we have calculated the observables and hence the Amati and Yonetoku relation are implemented to test the correlation of GRBs observables. For the two *Fermi* LAT/GBM detected GRBs (GRB150403A & GRB150314A), we considered unbinned likelihood analysis using the pass 8 data [9] to determine the probability of photons come from each event. Throughout the paper, we assume a flat-isotropic universe with $H_0 = 69.6$ km s^{-1} Mpc^{-1}, $\Omega_\Lambda = 0.714$ and $\Omega_m = 0.286$. Calculations of luminosity distances are done using the analytical approximation [10].

2. Sample and method of data analysis

We considered the GRBs detected by the *Fermi* satellite in 2015 with known redshift. In this sample, there are 5 long GRBs (observed duration > 2 s). Among these (GRB150403A & GRB150314A) are detected by both LAT and GBM while the other three sources (GRB150727A, GRB151027A & GRB150301B) are detected only by GBM as shown in Table 1. The highest-energy photons (E_{max}) in the LAT-detected GRBs with known redshift range between 0.1 GeV to more than 30 GeV. The highest-energy photons of the GRB150314A is ∼0.62 GeV (with 97.8 % photon probability) and GRB150403A is ∼5.4 GeV (with 99.6 % photon probability) belongs to the event which is observed at ∼81 s and ∼632 s after the GBM trigger, respectively. The GBM light curve of both GRB150314A and GRB150403A shows a bright single pulse with a duration T_{90} [11] of about 10.7 s and 22.3 s with energy range computed between 50 and 300 keV, respectively. The GBM light curve of GRB150301B consists of one main peak, the GRB150727A light curve shows a FRED-like (fast-rise exponential-decay) pulse and the GRB151027A light curve consists of three pulses with a duration T_{90} of about 13 s, 50 s and 124 s, respectively as shown in Table 1.

Table 1. Data on *Fermi* LAT/GBM detected GRBs with known redshift.

GRB	z	T_{90}(s)[f]	Best on-ground location	Prob. $> 90\%$ [l]	Detectors
150314A	1.758[a]	10.7	(RA, Dec)=125.40, 64.46[g]	9	*Fermi*-LAT/GBM
150403A	2.06[b]	22.3	(RA, Dec)=311.79, -62.76[h]	6	*Fermi*-LAT/GBM
150301B	1.517[c]	13	(RA, Dec)=89.157, -57.977[i]	-	*Fermi*-GBM
150727A	0.313[d]	50	(RA, Dec)=203.99, -18.355[j]	-	*Fermi*-GBM
151027A	0.81[e]	124	(RA, Dec)=272.491, 61.381[k]	-	*Fermi*-GBM

[a]de Ugarte Postigo A., et al., 2015, (GCN 17583)
[b]Pugliese V., et al., 2015, (GCN 17672)
[c]Lien Y., et al., 2015, (GCN 17515)
[d]Watson M., et al., 2015, (GCN 18089)
[e]Perley A., et al., 2015, (GCN 18487)
[f]The time between accumulating 5% & 95% of the counts associated with the GRB
[g]Axelsson M., et al., 2015, (GCN 17576)
[h]Longo F., et al., 2015, (GCN 17667)
[i]de Ugarte Postigo A., et al., 2015, (GCN 17523)
[j]Cenko B., et al., 2015, (GCN 18076)
[k]Maselli A., et al., 2015, (GCN 18478)
[l]Photons with probability $> 90\%$ above 100 MeV

2.1. Spectral analysis

For the time-integrated spectral analysis, data from the optimal sodium iodide (NaI) detectors were fitted together with bismuth germanate (BGO) detectors [12]. As in most of the previous

spectral analysis of GRBs, we used SBPL, Power-law function with an exponential high-energy cutoff [Comptonized (Comp)], Band function (Band) [8] and PL models. For the triggers selection, the criterion adopted in Guiriec et al. [13] is implemented. To perform the spectral analysis, the recently released software RMFIT (*v3.3pr7*) [14] tool kits has been used. The NaI data from ∼10 keV to ∼915 keV and the BGO data from ∼250 keV to ∼39 MeV are used by cutting out the overflow low and high-energy channels as well as the K-edge from ∼30 to ∼40 keV. The background in each of the GBM detectors was estimated by fitting polynomial functions to the light curves in various energy ranges before and after the source active time period. For GBM data, the background was fitted to the CSPEC data which cover a much longer time range, making the estimation of the background more reliable for long GRBs [15]. For GRB151027A, GRB150727A, GRB150403A, GRB150314A and GRB150301B, the triggers (n0+n1+n3+b0), (n0+n3+n4+b0), (n3+n4+b0), (n0+n1+n2+n9+na+b0) and (n0+n3+n4+n6+n7+n8+b0+b1) are used for the time-integral analysis for the time section T_{90} [11] and T_{peak} (the time at high peak count rate), respectively.

3. Data analysis

The spectral parameters in Tables 2 and 3 have been obtained through the analysis of the time-integrated spectrum extracted from the GBM data by performing the software package RMFIT (version 8.1) for the duration of T_{90} and T_{peak} in the ∼10 keV to ∼39 MeV energy range, respectively. The best spectral parameter values were estimated by optimizing the Castor C-statistic (hereafter C-stat), which is a likelihood technique that converges to χ^2 for a specific data set when there are enough counts. We have selected the best model by choosing the fit with the lowest C-stat value after each of the spectrum fitted with a Band, PL, SBPL and Comp models. Table 2 and 3 shows the results of these fits. Table 2 lists 5 long GRBs with their time integrated spectral parameters (Column 3, 4, and 7) and the time integrated isotropic radiated energy, computed in the rest frame in the 1 keV - 10 MeV energy range (E_{iso}, Column 5) and derived intrinsic peak-energy (E^i_{peak}, Column 6). Table 3 contains, the spectral analysis of five long GRBs for T_{peak} with the obtained parameters (Column 3, 4, and 5) and derived intrinsic peak luminosity, computed in the rest frame in the 1 keV - 10 MeV energy range (L_{iso}, Column 6). Figure 1 and 2 show the Band spectrum fit of GBM data of GRB150403A & GRB150314A,

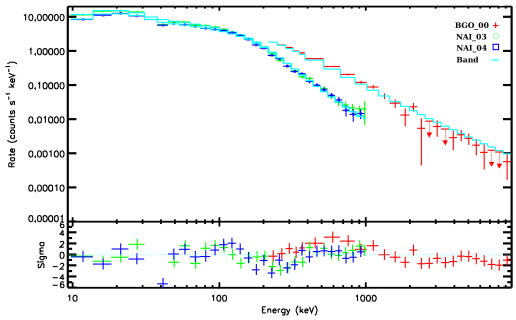

Figure 1. The time-integrated spectrum of GRB150403A fitted by a Band function.

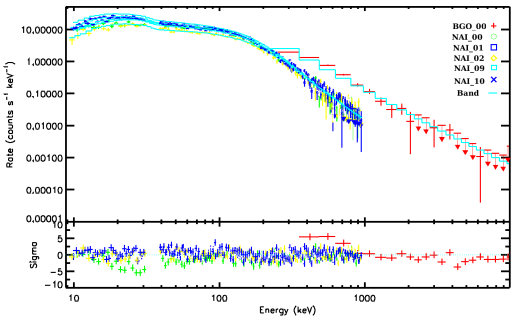

Figure 2. The time-integrated spectrum of GRB150314A fitted by a Band function.

respectively. These bursts are detected by both the LAT and GBM. As shown in Tables 2 and 3, the GRB150403A and GRB150314A show a high band model component and their observed peak energies are the largest of the sample. In tables 2 & 3, the associated errors reported on E_{iso}, L_{iso} and E^i_{peak} was computed by properly weighing for data uncertainties [16] except for GRB150314A, we assume 10% error in these measurements due to some statistical errors on the parameters.

Table 2. Results of the spectral fits for the duration of T_{90} and derived E_{iso} in the GRB rest frame.

GRB	T_{90} [sec.]	α/Index1	β/Index2	$E_{iso}/10^{52}$ [erg]	E^{i}_{peak} [keV]	E_{peak}[keV]	Model	C-stat/dof
151027A	-2.048 - 133.120	-1.47 ± 0.039	-	2.99 ± 0.365	592.6±112.9	327.4 ± 62.4	Comp	866.55/430
		-1.46 ± 0.06	-1.98 ± 0.12	-	-	-	SBPL	863.56/429
		-1.66 ± 0.02	-	-	-	-	PL	908.54/431
150727A	0.003 - 50.177	-0.38±0.20	-2.18±0.21	0.32 ± 0.14	224.3 ± 37.7	170.8 ± 27.2	Band	1060.0/424
		-0.59±0.12	-	-	-	220.8 ± 19.5	Comp	1066.6/425
		-0.58±0.2	-2.19±0.19	-	-	-	SBPL	1060.3/424
		-1.48 ± 0.02	-	-	-	-	PL	1191.3/426
150403A	-0.512 - 23.04	-0.77 ± 0.02	-2.04 ± 0.04	93.52 ± 4.46	1172.6 ± 43.1	383.2 ± 14.1	Band	438.65/315
		-0.88 ± 0.01	-	-	-	531.3 ± 13.4	Comp	550.79/316
		-0.87 ± 0.02	-1.99 ± 0.03	-	-	-	SBPL	434.55/315
		-1.37 ± 0.004	-	-	-	-	PL	4113.5/317
150314A	-2.912 - 11.424	-0.58 ± 0.01	-2.35 ± 0.04	87.4 ± 8.74	870.7 ± 87.1	315.7 ± 5.2	Band	1354.2/660
		-0.65 ± 0.008	-	-	-	367.6 ± 4.2	Comp	1467.6/661
		-0.73 ± 0.009	-2.25 ± 0.03	-	-	-	SBPL	1359.3/660
		-1.34 ± 0.003	-	-	-	-	PL	15663/662
150301B	-2.56 - 13.824	-1.13 ± 0.09	-2.21±0.25	3.64 ± 0.97	498.85 ± 98.16	198.2 ± 39.0	Band	963.3/857
		-1.19 ± 0.06	-	-	-	244.3 ±30.1	Comp	965.44/858
		-1.28 ± 0.06	-2.35± 0.29	-	-	-	SBPL	963.45/857
		-1.60 ± 0.02	-	-	-	-	PL	1043.3/859

Table 3. Results of the spectral fits for the duration of T_{peak} and L_{iso} in the GRB rest frame.

GRB	T_{peak} [sec.]	α	β	E_{peak}[keV]	L_{iso} [erg/s]	Model	C-stat/dof
151027A	0.002 - 1.792	-0.71± 0.096	-2.28±0.19	170.0 ± 19.9	0.36 ± 0.096	Band	439.14429
		-0.83± 0.06	-	208.7 ± 14.7	-	Comp	448.7/430
		-0.96± 0.07	-2.46±0.23	-	-	SBPL	439.06/429
		-1.52± 0.02	-	-	-	PL	664.73/431
150727A	4.096 - 6.144	-0.59 ± 0.31	-3.13±3.58	273.3 ± 89.4	-	Band	402.16/426
		-0.58 ± 0.28	-	273.9 ± 65.2	0.0101 ± 0.0053	Comp	402.24/427
		-0.89 ± 0.21	-4.35±5.42	-	-	SBPL	402.46/426
		-1.42± 0.056	-	-	-	PL	420.79/428
150403A	10.752 - 12.80	-0.66 ± 0.03	-2.14 ± 0.06	480.0 ± 26.4	20.55 ± 1.55	Band	338.08/294
		-0.79 ± 0.02	-	649.6 ± 24.6	-	Comp	424.79/295
		-0.77 ± 0.032	-2.08 ± 0.05	-	-	SBPL	339.86/294
		-1.38± 0.008	-	-	-	PL	1688.0/296
150314A	1.184 - 3.232	-0.296 ± 0.018	-2.4 ± 0.048	293.6 ± 5.6	22.2 ± 2.22	Band	1041.0/656
		-0.42 ± 0.01	-	352.3 ± 4.48	-	Comp	1159.7/657
		-0.49 ± 0.02	-2.32 ± 0.04	-	-	SBPL	1061.6/657
		-1.31± 0.004	-	-	-	PL	11083/658
150301B	1.536 - 3.584	-1.07 ± 0.12	-2.39 ±0.53	211.7 ± 50.4	0.55 ± 0.203	Band	933.9/856
		-1.13 ± 0.0.09	-	249.4 ± 40.5	-	Comp	934.2/857
		-1.21 ± 0.098	-2.34 ±0.37	-	-	SBPL	934.53/856
		-1.59± 0.03	-	-	-	PL	987.46/858

4. Correlation

4.1. Amati relation

In order to determine the strength and significance of each correlation, we utilized a linear regression analysis using the Pearson's and Spearman's correlation. The Amati relation is shown in Figure 3 for the *Fermi*-2015 sample and 68 GRBs data from the Amati et al., 2008 (A2008) [17] with measured redshift. The E_{iso} was determined in the rest-frame energy range from 1 keV to 10 MeV. The black dashed line is the power law best-fit (obtained by

weighting each point by its error on both E^i_{peak} and E_{iso}) of 5 *Fermi*-2015 GBM GRBs given by $E^i_{peak}[\mathrm{keV}] = (338.6 \pm 78.0)\,(E_{iso}/10^{52}\mathrm{erg})^{0.26\pm0.053}$ with the reduced $\chi^2_{red} = 3.14$. The Spearman's rank correlation coefficient is $\rho_{sp} = 0.9$ with the chance probability $P_{sp} = 0.037$. The combination of *Fermi*-2015 and A2008 data are fitted together by power law (magenta solid line) $E^i_{peak}[\mathrm{keV}] = (93.1 \pm 6.23)\,(E_{iso}/10^{52}\mathrm{erg})^{0.56\pm0.02}$ with the reduced $\chi^2_{red} = 6.69$ and the $\rho_p = 0.70$ with P_p shows an extremely low value of 4.34×10^{-12}. The ρ_{sp} is 0.85 with the $P_{sp} = 2.324 \times 10^{-21}$. In Figure 3, the A2008 data (GRB150727A) with smaller E_{iso} and E^i_{peak} is seems an outliers of the correlation.

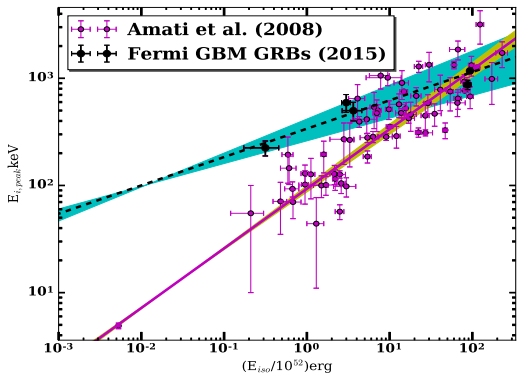

Figure 3. The E^i_{peak} - E_{iso} relation. The black circles are our present results of five long *Fermi* GRBs. The data from A2008 [17] are shown by the magenta circles. Both results are plotted as E^i_{peak} at the rest frame of the GRBs and the E_{iso} is calculated using the T_{90} fluence.

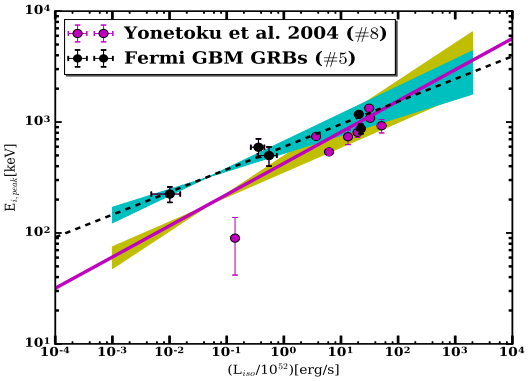

Figure 4. The E^i_{peak} - L_{iso} relation. The black circles are our present results with five *Fermi* GRBs. The results of Yonetoku et al., 2004 (Y2004) [3] is also shown as the magenta circles. Both results are plotted as E^i_{peak} at the rest frame of the GRBs and the peak luminosity derived from the time T_{peak} flux.

Make plots bigger!

4.2. Yonetoku relation

Another correlation among observable quantities is between E^i_{peak} and L_{iso} (Yonetoku correlation). The correlation defining L_{iso} as the luminosity emitted at the peak of the light curve. In Figure 4, we show the peak luminosities, as a function of intrinsic peak energy in the rest frame of each GRB. We combined our *Fermi*-2015 GRBs data with the 8 BATSE Y2004 [3] results in the same plane. This is another key result of the present work. In Y2004 data, the redshift of GRB980326 and GRB980329 are not precisely determined and only the upper limit of intrinsic peak energy has been reported for GRB980703. Therefore, we can exclude these three bursts from our data analysis to avoid inaccurate result. When we adopt the power-law model to the E^i_{peak} - L_{iso} relation, the best-fit function (magenta solid line) of 5 *Fermi*-2015 data is $E^i_{peak}[\mathrm{keV}] = (598.4 \pm 76.9)\,(L_{iso}/10^{52}\mathrm{ergs}^{-1})^{0.20\pm0.04}$ with the reduced $\chi^2_{red} = 3.66$. The Spearman's rank linear correlation coefficient is 0.8 with chance probability 0.104. The best power-law fit (magenta solid line) for the *Fermi*-2015 data (black circles) together with Y2004 data (magenta circles) is $E^i_{peak}[\mathrm{keV}] = (424.2 \pm 70.96)\,(L_{iso}/10^{52}\mathrm{ergs}^{-1})^{0.28\pm0.06}$ with the reduced $\chi^2_{red} = 8.3$. The Pearson's correlation coefficient is ($\rho_p = 0.74$ and the chance probability shows $P_p = 0.0036$). The Spearman's rank correlation coefficient is $\rho_{sp} = 0.89$ with the low chance probability $P_{sp} = 4.565 \times 10^{-5}$.

black dashed line

5. Discussion

We studied the time-integrated spectra of five *Fermi* GBM GRBs by fitting the light curve over the duration of T_{90} and T_{peak} in the 10 keV - 39 MeV energy range, respectively. The spectral parameters obtained from this analysis are reported in Tables 2 and 3, where the Band function considered as adequately fitting GRB spectra. For the *Fermi*-2015 GRBs observables, we found a high correlation of peak energy with isotropic radiated energy and the peak luminosity on the GRB source frame. For the *Fermi*-2015 data, there is a higher and tighter correlation between E^i_{peak} and E_{iso}. Their best-fit power law index is 0.26 ± 0.053 with the reduced $\chi^2_{red} = 3.14$. This looks considerably tighter and more reliable than the relations suggested by the previous works [18, 19]. The best-fit power law index for the *Fermi*-2015 and A2008 joined data is 0.56 ± 0.02 with the reduced $\chi^2_{red} = 6.69$, which has a similar result with the previous Amati [17] correlation (i.e. the index of the power-law, $\sim$0.57 and $\chi^2_{red} = 7.2$). The Spearman's rank correlation coefficient also shows a high correlation between the observables E^i_{peak} and E_{iso} (ρ_{sp} = 0.9). As shown in Fig. 4, the *Fermi*-2015 and Y2004 data are poorly fitted by the power low with reduced $\chi^2_{red} = 8.3$. This indicates that the fit has not fully captured the relationship between the observables data. However, the Pearson's correlation coefficient ($\rho_p = 0.74$) and the Spearman's rank correlation coefficient ($\rho_{sp} = 0.89$) are indicating a positive strong correlation. For the L_{iso} - E^i_{peak} correlation analysis, our results are limited by the small number of GRBs in the sample: we have 13 GRBs in total. To get a more reliable conclusion, the number of GRBs with well-determined redshifts and spectra needs to be significantly expanded.

Acknowledgments

The *Fermi*-LAT Collaboration acknowledges support for LAT development, operation and data analysis from NASA and DOE (United States), CEA/Irfuand IN2P3/CNRS (France), ASI and INFN (Italy), MEXT, KEK, and JAXA (Japan), and the K.A. Wallenberg Foundation, the Swedish Research Counciland the National Space Board (Sweden). Science analysis support in the operations phase from INAF (Italy) and CNES (France) is also gratefully acknowledged. The work presented in this paper was supported in part by an MWGR 2015 grant from the National Research Foundation with Grant No. 93273.

References

[1] Piran T 1999 *Phys.Rept.* **314** 575
[2] Amati L 2006 *MNRAS* **372** 233
[3] Yonetoku D *et al.* 2004 *ApJ* **609** 935
[4] Amati L *et al.* 2002 *A&A* **390** 81
[5] Heussaff V, Atteia J L and Zolnierowski Y 2013 *A&A* **557** A100
[6] Ghirlanda G *et al.* 2012 *MNRAS* **422** 2553
[7] Nava L, Ghirlanda G and Ghisellini G 2009 *arXiv preprint arXiv:0902.1522*
[8] Band D *et al.* 1993 *ApJ* **413** 281
[9] Atwood W *et al.* 2013 *ApJ* **774** 76
[10] Wright E L 2006 *ASP* **118** 1711
[11] Ackermann M *et al.* 2010 *ApJ* **716** 2
[12] Meegan C *et al.* 2009 *ApJ* **702** 791
[13] Guiriec S *et al.* 2010 *ApJ* **727** L33
[14] *http://fermi.gsfc.nasa.gov/ssc/data/analysis/rmfit/*
[15] Guiriec S *et al.* 2015 *ApJ* **807** 148
[16] Bevington J 1969 *McGrawHill* 36
[17] Amati L *et al.* 2008 *ApJ* **390** 81
[18] Dirirsa F F and Razzaque S 2015 *PoS(SSC2015)066*
[19] Amati L 2005 *MNRAS* **372** 233